

## Theoretical determination of stress around a tensioned grouted anchor in rock

Alan Showkati, Parviz Maarefvand\* and Hossein Hassani

Faculty of Mining and Metallurgical Engineering, Amirkabir University of Technology,  
424 Hafez Avenue, P.O. Box 15875-4413, Tehran, Iran

(Received January 29, 2014, Revised December 05, 2014, Accepted December 20, 2014)

**Abstract.** A new theoretical approach for analysis of stress around a tensioned anchor in rock is presented in this paper. The solution has been derived for semi-infinite elastic rock and anchor and for plane strain conditions. The method considers both the anchor head bearing plate and its grouted bond length embedded in depth. The solution of the tensioned rock anchor problem is obtained by superimposing the solutions of two simpler but fundamental problems: A distributed load applied at a finite portion (bearing plate area) of the rock surface and a distributed shear stress applied at the anchor-rock interface along the bond length. The solution of the first problem already exists and the solution of the shear stress distributed along the bond length is found in this study. To acquire a deep understanding of the stress distribution around a tensioned anchor in rock, an illustrative example is solved and stress contours are drawn for stress components. In order to verify the results obtained by the proposed solution, comparisons are made with finite difference method (FDM) results. Very good agreements are observed for the theoretical results in comparison with FDM.

**Keywords:** tensioned anchors; elastic rock; stress distribution; theoretical solution; bond length; bearing plate

---

### 1. Introduction

A tensioned anchor is a structural element installed in rock or soil to reinforce it or to transfer an applied tensile load from a structure to surrounding ground. The earliest reports of anchoring tendons into the rock to secure a roof date from 1918 in the Mir Mine of Upper Silesia in Poland (Littlejohn 1993). In the field of civil engineering the history of rock anchors dates from 1934 when Coyne pioneered their use during the raising of the Cheurfas Dam in Algeria (Littlejohn 1993). Since 1934 there has been a huge increase in the use of anchorages throughout the world, and millions of rock anchors have been installed for various engineering purposes.

Nowadays, rock anchors are employed to solve problems involving direct tension, sliding, overturning, and ground prestressing. For example, tensioned rock anchors are used to reinforce high slopes and deep urban excavations (Littlejohn *et al.* 1977, Sagaseta *et al.* 2001, Akgün and Koçkar 2004, Kim *et al.* 2007, Tonon and Asadollahi 2008, Sabatini *et al.* 1999), anchoring of tension foundations into the ground (Saliman and Schaefer 1968, Hanna 1982, Wyllie 2005,

---

\*Corresponding author, Ph.D., E-mail: [parvizz@aut.ac.ir](mailto:parvizz@aut.ac.ir)

Danziger *et al.* 2006), stabilization and improvement of overturning resistance in concrete dams (Bruce 1997), retaining walls (Sabatini *et al.* 1999, Bruce 1992), pile testing, bridges, tunnels, underground caverns (Littlejohn 1993).

The basic components of a rock anchor are (see Fig. 1): (i) anchor head; (ii) unbonded length; and (iii) bond length (Sabatini *et al.* 1999). The anchor head is a component that is capable of transmitting the tensile load from the anchor to the surface of rock or structure requiring support. The purpose of the bond length is to transfer the anchor tensile load to the surrounding ground. The unbonded length of the tendon transmits the tensile load from the bond length to the anchor head (Littlejohn 1993). The anchor tendon is comprised of steel bar or strand/wire which is secured to the rock with cement or epoxy grout (Sabatini *et al.* 1999).

Tensioning is the special characteristic of rock anchors by which a particular load is applied to the surrounding ground. Tensioned anchors alter the primary state of stress in the ground by developing shear stresses along the bond length and by compressive stresses applied through the bearing plate (i.e., the anchor head).

As the tendon is put in tension, the rock anchor provides confinement to the medium between its two ends (Bobet and Einstein 2011). Moreover, according to the Mohr-Coulomb failure criterion, the confinement induced by rock anchors increases minimum principal stress ( $\sigma_3$ ) in the ground which in turn increases the strength of surrounding rock. Tensioned anchors also strengthen jointed rock masses by increasing the frictional resistance along discontinuities (Littlejohn 1993).

The design of rock anchors demands a good understanding of their action mechanism and interaction with the surrounding rock. This demands accurate estimation of stresses induced by rock anchors in the rock mass. Culver and Jorstad (1967) stated that in mechanically anchored rockbolts there are extremely high local stresses in the anchor region which are capable of generating fractures in rock. They also pointed out that the knowledge of magnitude and distribution of stress is essential in describing the conditions which would initiate large fractures in the surrounding rock mass. Generally, accurate estimation the stress around tensioned rock anchors provides basic insight into their behavior which eventually leads to improved designs. To achieve this goal various methods may be used like experimental observations, numerical analyses and analytical solutions.

Hobst and Zajic (1977) discussed the problem of stress distribution around anchors using model tests of a tensioned anchor in sand. They found that there is a zone of compression at the proximal end and a zone of tension at the distal end of the anchor.

Nitzsche and Haas (1976) and Gao and Kang (2008) investigated numerically the effect of tensioned rockbolts on the state of stress around roof bolts in underground openings. Yap and Rodger (1984) also studied the behavior of vertical rock anchors using finite element method (FEM). Although numerical approaches are widely used to simulate various geomechanical problems, they suffer two major weaknesses in modelling tensioned anchors. In fact, numerical methods are incapable of considering the bearing plate effects and real distribution and magnitude of shear stresses mobilized along the tendon-grout-rock interfaces. These shear stresses, as will be shown later, can greatly influence the magnitude and distribution of stresses around tensioned rock anchors.

Two important fundamental solutions derived from the theory of elasticity that are especially relevant to the study of anchors are: (1) Boussinesq solution (Poulos and Davis 1974), for a point load at the surface of an infinite half-space; and (2) Mindlin solution (Mindlin 1936), for a point load at the interior of a semi-infinite medium. In this regard, Wijk (1978) and Wu *et al.* (2010)

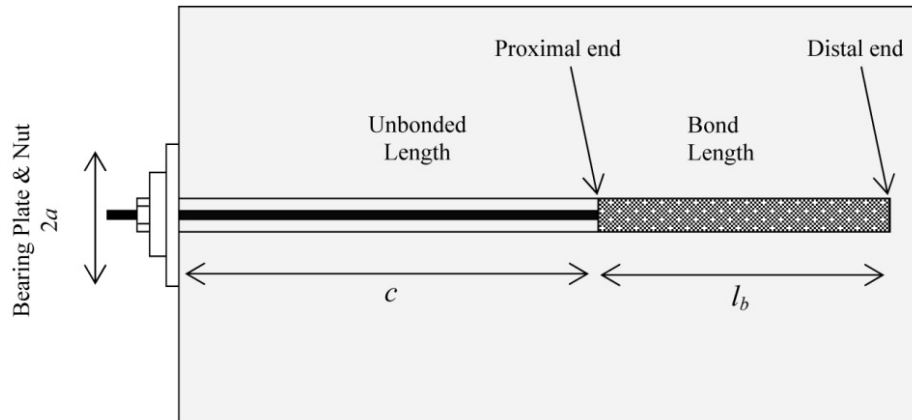


Fig. 1 Schematic diagram of a tensioned rock anchor

used a combination of the abovementioned solutions together with the principle of superposition (Timoshenko and Goodier 1970) to obtain analytic solutions for stresses around tensioned rockbolts. They assumed that a tensioned rockbolt can be modeled by a pair of equal point loads of opposite direction. Moreover, Papanastassopoulou (1983) presented a closed form solution for stress field around tensioned bolts in homogeneous and linear elastic rock mass using a pair of infinite tangential line loads.

Culver and Jorstad (1967) and Russell (1968) obtained two-dimensional elastic solutions for stresses around mechanically anchored (cone-type) and expansion-type rockbolts, respectively. They used models which consist of surface tractions (normal and/or shear) applied at a limited borehole surface. Furthermore, Bray in (Brown 1987) discussed the influence of a tensioned rockbolt on the stress distribution around a circular opening.

While limited in their applicability due to some of the assumptions made in their derivation, analytic solutions provide the means for a quick quantitative estimate of the interaction between the rock mass and the anchor. All analytical solutions proposed so far to obtain the stress field around tensioned anchors ignore the existence of bearing plate and bond length in their derivation. In fact, to the knowledge of authors, no analytical solution exists that accounts for the contribution of bearing plate and shear stress mobilization along the bond length to the change of stresses in the surrounding rock.

This paper presents a theoretical approach for the analysis of tensioned grouted anchors in rock considering the presence of bearing plate and bond length at depth. Due to complexities associated with the behavior of rock mass, the most common approach which can be adopted to ease the problem is to assume that the rock is homogeneous, isotropic with a linear elastic constitutive relationship between stress and strain for the rock material. This approach has proven (Windsor and Thompson 1993, Brown 1974) to be useful particularly in predicting zones of stress concentration and stress relaxation near excavations which are relevant in this study. Thus, for the derivation of the solution the following assumptions are made:

- (i) Linear elastic behavior of rock mass and rock anchor
- (ii) Semi-infinite rock mass surrounding the anchor.
- (iii) Plane strain condition in the direction perpendicular to the cross-section of the anchor (Fig. 1)

In addition, to highlight stresses induced by the tensioned anchor, the surrounding rock is assumed to be weightless with no in-situ stresses.

An illustrative example is given at the end of this paper to investigate the stress distribution around a tensioned rock anchor. To verify the proposed elastic solutions, a number of continuum-based numerical analyses are performed with the finite-difference method (FDM) program, and results are compared with those of theoretical approach.

## 2. Methodology

In this section the methodology used to obtain a solution for stress distribution around tensioned rock anchors is discussed. Fig. 1 shows a schematic of the tensioned rock anchor problem that will be solved. It consists of a rock anchor installed at the surface of a semi-infinite elastic rock mass. The rock anchor is tensioned and locked-off at the load  $T$ . As proposed by Windsor (1997), a reinforcing system is comprised of the ground, the reinforcing element (steel rod/strands), the internal fixture and the external fixture. For grouted rock anchors, the external fixture refers to the bearing plate and nut and the internal fixture is a medium such as cement grout or resin which provides a coupling condition at the interface.

Since rock anchors are considered as springs of constant stiffness with load proportional to elongation, a tensioned anchor can be replaced by two loads acting at the positions of external and internal fixtures. In literature, some authors replaced external and internal fixtures with point loads (see for example: Wijk (1978), Papanastassopoulou (1983), Wu *et al.* (2010)) and some used distributed loads as internal fixture (see for example: Culver and Jorstad (1967), Russell (1968)). Since the anchor head is represented by a point load in previous works, the bearing plate influence on the stress distribution is ignored. Moreover, in the case of grouted anchors, real distribution of shear stresses mobilized along the bond length (internal fixture) should also be considered in the analysis.

In this study, both the anchor bearing plate and its bond (embedding) length are considered for analysis of stress. The bearing plate can be modeled by a uniform load as the anchor load is distributed by the bearing plate over the rock surface. Furthermore, the tensile load transferred to the surrounding rock through the bond length can be simulated by shear stresses mobilized at the rock-anchor interface.

Since all differential equations and boundary conditions are linear in the theory of elasticity (Timoshenko and Goodier 1970), the anchor problem can be decomposed into two simpler but fundamental problems. Specifically, two fundamental solutions relevant to the problem of tensioned anchors are:

- (1) A uniform distributed load of magnitude  $q$  applied over a finite portion surface of a semi-infinite rock (Fig. 2(a)),
- (2) A non-uniform distribution of shear stress applied at the interface of the rock-anchor along the bond length (Fig. 2(b)).

Fig. 2 illustrates the geometry of the decomposed tensioned anchor problem. Since this is a two-dimensional elastic analysis, it is supposed that the anchor loads are distributed per unit width of the semi-infinite medium. The solution of the anchor problem shown in Fig. 1 can be obtained by superposition of the solutions of the fundamental problems. In the following sections, the solutions of these fundamental problems are found first and then, a comprehensive analysis of

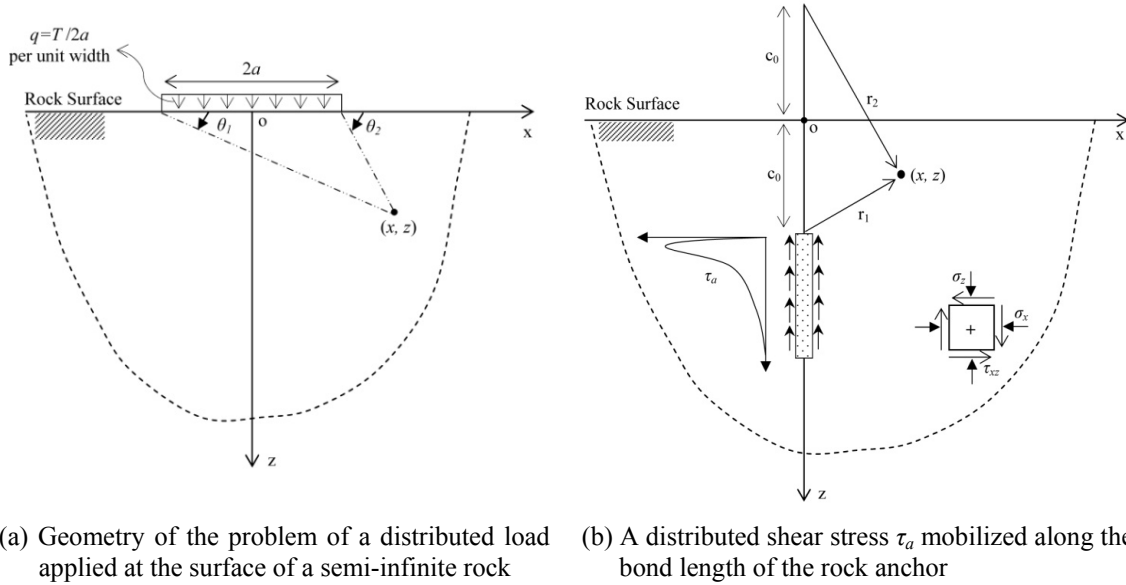


Fig. 2 Problem decomposition

stress is also presented. Note that in this paper compression is taken as positive and tension as negative.

### 3. Solution of fundamental problems

#### 3.1 A distributed load at the surface of a semi-infinite rock

In this section the effect of anchor load distributed by the bearing plate is considered. In order to model the bearing plate in the analysis, a uniform pressure corresponding to the load distributed by the bearing plate should be applied at the rock surface. The geometry of the problem of distributed load applied at the surface of a semi-infinite medium is illustrated in Fig. 2(a). The solution of this problem is available in Sadd (2005). Thereupon, the stresses produced under a distributed load,  $q$ , over a finite portion ( $-a < x < a$ ) of the surface of a semi-infinite rock are

$$\sigma_x = \frac{q}{2\pi} [2(\theta_2 - \theta_1) + (\sin 2\theta_2 - \sin 2\theta_1)] \tag{1}$$

$$\sigma_z = \frac{q}{2\pi} [2(\theta_2 - \theta_1) - (\sin 2\theta_2 - \sin 2\theta_1)] \tag{2}$$

$$\tau_{xz} = \frac{q}{2\pi} [\cos 2\theta_2 - \cos 2\theta_1] \tag{3}$$

Where  $q$  is the magnitude of the distributed load  $[FL^{-2}]$  at the rock surface. Other parameters

are defined in Fig. 2(a). Note that  $\theta_1$  and  $\theta_2$  are in radians.

### 3.2 A non-linear distribution of shear stress along the bond length

In examining the behavior of a tensioned rock anchor, it is necessary to determine the distribution of shear stress on an anchor element which when used in conjunction with elastic theory leads to a mathematically tractable solution.

In order to obtain a solution for the problem of a distributed shear stress applied to the rock along the anchor bond length, a simpler but essential solution has to be introduced first. The solution of a point load problem acting at a specific distance from the surface of a semi-infinite medium is relevant here. On the other hand, a solution is also needed for modeling the real interaction between anchor and rock. In the subsequent sections, the abovementioned solutions are presented and the stresses induced by a non-linear distribution of shear stress along the bond length are also obtained.

#### 3.2.1 A point load in a semi-infinite rock

This problem, known as Mindlin's Problem consists of a concentrated force  $P$  applied at a point in the interior of a semi-infinite medium (see Fig. 3). A two-dimensional plane-stress solution for Mindlin's problem is developed by Melan in (Poulos and Davis 1974). After some modifications for plain strain conditions and particular geometry of the interested problem in Fig. 3, Melan's solution is expressed as follows

$$\sigma_x = \frac{-P}{\pi} \left[ \frac{1-\nu}{2(1-2\nu)} \left( \frac{(z-c)x^2}{r_1^4} + \frac{(z+c)(x^2+2cx^2)}{r_2^4} - \frac{8cz(z+c)x^2}{r_2^6} \right) + \frac{1-3\nu}{4(1-2\nu)} \left( -\frac{(z-c)x^2}{r_1^2} + \frac{z+3c}{r_2^2} - \frac{4zx^2}{r_2^4} \right) \right] \quad (4)$$

$$\sigma_z = \frac{-P}{\pi} \left[ \frac{1-\nu}{2(1-2\nu)} \left( \frac{(z-c)^3}{r_1^4} + \frac{(z+c)[(z+c)^2+2cz]}{r_2^4} - \frac{8cz(z+c)x^2}{r_2^6} \right) + \frac{1-3\nu}{4(1-2\nu)} \left( \frac{z-c}{r_1^2} + \frac{3z+c}{r_2^2} - \frac{4zx^2}{r_2^4} \right) \right] \quad (5)$$

$$\tau_{xz} = \frac{-Px}{\pi} \left[ \frac{1-\nu}{2(1-2\nu)} \left( \frac{(z-c)^2}{r_1^4} + \frac{(z^2-2cz-c^2)}{r_2^4} + \frac{8cz(z+c)^2}{r_2^6} \right) + \frac{1-3\nu}{4(1-2\nu)} \left( \frac{1}{r_1^2} - \frac{1}{r_2^2} - \frac{4z(z+c)}{r_2^4} \right) \right] \quad (6)$$

where

$$r_1^2 = x^2 + (z-c)^2$$

$$r_2^2 = x^2 + (z+c)^2$$

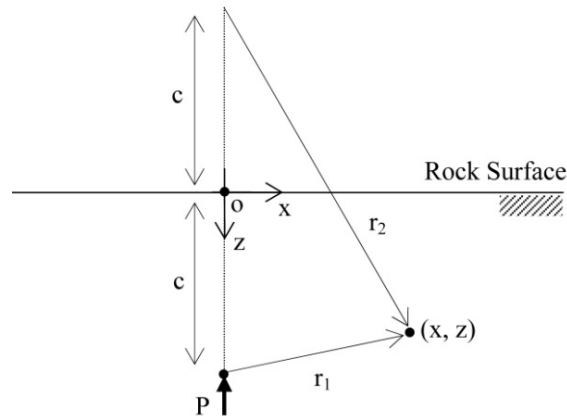


Fig. 3 A concentrated load of magnitude  $P$  applied at the distance  $c$  from the surface of a semi-infinite rock

$\nu$  is the Poisson's ratio of the rock.

### 3.2.2 Modeling rock-anchor interaction

When a tensile force is applied to the anchor's tendon, it is transferred to the grout through shear stresses mobilized at the tendon/grout interface. To investigate the influence of these shear stresses on the stresses produced around a rock anchor, it is necessary to determine the distribution of shear stress mobilized along the anchor's shaft.

The transfer of the anchor load,  $T$ , to the surrounding rock is a complicated problem and no exact solution exists in this regard. Shear-lag approach, which is often used for analysis of stress transfer problems in composite materials or materials with inclusions, can be applied to determine an approximate solution (McCartney 1989, Hseuh 1995, Narin and Mendels 1996). Several authors (see for example, Farmer 1975, Li and Stillborg 1999) applied the shear-lag method to obtain an analytical solution for shear stresses developed at the grouted length of rockbolts. The solution proposed by Li and Stillborg (1999) is more general than others and has shown good agreement with experiments (Bobet 2006).

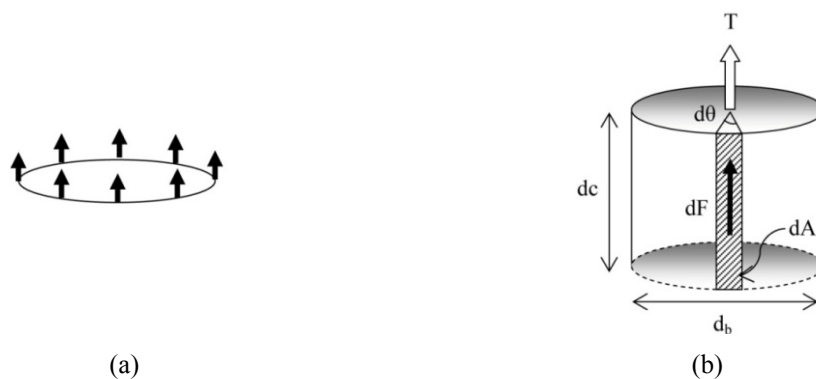


Fig. 4 (a) A ring of concentrated load applied at the perimeter of the tendon; (b) Schematic of a small element of the anchor tendon

For grouted rock anchors subjected to a tensile stress, attenuation of the shear stress,  $\tau_a$ , along the bond length before any tendon/grout interface decoupling is expressed as (Li and Stillborg 1999)

$$\tau_a(z) = \frac{\alpha}{2} \cdot \sigma_a \cdot \exp\left(-2\alpha \frac{z}{d_b}\right) \quad (7)$$

where

$$\alpha^2 = \frac{2G_r G_g}{E_b \left[ G_r \ln\left(\frac{d_g}{d_b}\right) + G_g \ln\left(\frac{d_0}{d_g}\right) \right]}$$

$$G_r = \frac{E_r}{2(1+\nu_r)}; \quad G_g = \frac{E_g}{2(1+\nu_g)}$$

$\sigma_a$  is the axial tensile stress of the anchor at the loading point,  $z$  is the distance from the proximal end of the bond length,  $d_b$  is the diameter of the tendon,  $d_g$  is the diameter of the borehole (grout cylinder),  $d_0$  is the diameter of the anchor influence area, which can be estimated as  $d_0 = 10 d_g$  (Li and Stillborg 1999),  $E_b$  is Young's modulus of the tendon steel,  $E_r$  is Young's modulus of the rock,  $E_g$  is Young's modulus of the grout,  $\nu_r$  and  $\nu_g$  are the Poisson's ratio of the rock and grout, respectively.

According to Eq. (7), the shear stress is maximum at the proximal end and quickly declines along the bond length due to the negative exponent. The shape of the shear stress  $\tau_a$  distribution suggested by Li and Stillborg (1999) in Eq. (7) is shown in Fig. 2(b).

As stated earlier, the mobilized shear stress is applied over the circumference of the anchor shaft at the tendon/grout interface. As the section of the anchor shaft element is circular, the shear stress on the interface can be regarded as a concentrated ring load in vertical direction (Fig. 4(a)). The relationship between the force in the tendon inside the bonded zone,  $dF$ , and the shear stress at the interface can be established by considering a small section of the tendon as shown in Fig. 4(b). Regarding Fig. 4, the following expressions can be derived.

$$dF = \tau_a dA = \tau_a \cdot \frac{d_b}{2} \cdot dc \cdot d\theta \quad (8)$$

$$\sigma_a = \frac{4T}{\pi d_b^2} \quad (9)$$

From Eqs. (7)-(9), the anchor force,  $dF$ , can be obtained as below

$$dF = \frac{4T}{\pi d_b} \cdot \exp\left(-2\alpha \frac{z}{d_b}\right) \cdot dc \cdot d\theta \quad (10)$$

According to the definitions of  $z$  in Eq. (7),  $c_0$  in Fig. 2(b) and  $c$  in Fig. 3, the distance from the proximal end of bond length,  $z$ , can be redefined as  $(c - c_0)$ . Therefore, integration of Eq. (10) with respect to the argument ( $d\theta$ ) from 0 to  $2\pi$  yields the following equation for a ring of  $dF$

$$dF = \frac{2\alpha T}{d_b} \cdot \exp\left(-2\alpha \frac{(c-c_0)}{d_b}\right) dc \quad (11)$$

The stress components caused by a unit load ring of  $dF$  at an arbitrary point,  $(x,z)$ , in the surrounding rock can be obtained using Eqs. (4)-(6) where  $P$  is replaced by  $dF$  from Eq. (11). Integration of the resulting stress components with respect to  $dc$  from  $c_0$  to  $c_0 + l_b$  leads to the stresses caused by the exponential distribution of shear stress applied along the anchor bond length (see Appendix A. for details of the derivation of the equations).

#### 4. Development of the analytical solution

As stated earlier, the Superposition Principle is used for derivation of the stress formulae. The stresses at a particular point,  $(x,z)$ , are obtained by addition of the stress components found from the solution given in Section 3.1 (Eqs. (1)-(3)) and the solution proposed in Section 3.2 for stresses around the anchor bond length. Accordingly, the complete solution of the post-tensioned grouted rock anchor with bearing plate is expressed as follows

$$\begin{aligned} \sigma_x = & \int_{c_0}^{c_0+l_b} \left( \frac{ABT}{\pi} \cdot \exp[A(c-c_0)] \right) \left( \frac{(z-c)x^2}{r_1^4} + \frac{(z+c)(x^2+2cx^2)-2cx^2}{r_2^4} - \frac{8cz(z+c)x^2}{r_2^6} \right) dc \\ & + \int_{c_0}^{c_0+l_b} \left( \frac{ACT}{\pi} \cdot \exp[A(c-c_0)] \right) \left( -\frac{(z-c)}{r_1^2} + \frac{z+3c}{r_2^2} - \frac{4zx^2}{r_2^4} \right) dc \\ & + \frac{T}{4\pi a} [2(\theta_2 - \theta_1) + (\sin 2\theta_2 - \sin 2\theta_1)] \end{aligned} \quad (12)$$

$$\begin{aligned} \sigma_z = & \int_{c_0}^{c_0+l_b} \left( \frac{ABT}{\pi} \cdot \exp[A(c-c_0)] \right) \left( \frac{(z-c)^3}{r_1^4} + \frac{(z+c)[(z+c)^2+2cz]}{r_2^4} - \frac{8cz(z+c)x^2}{r_2^6} \right) dc \\ & + \int_{c_0}^{c_0+l_b} \left( \frac{ACT}{\pi} \cdot \exp[A(c-c_0)] \right) \left( \frac{z-c}{r_1^2} + \frac{3z+c}{r_2^2} - \frac{4zx^2}{r_2^4} \right) dc \\ & + \frac{T}{4\pi a} [2(\theta_2 - \theta_1) - (\sin 2\theta_2 - \sin 2\theta_1)] \end{aligned} \quad (13)$$

$$\begin{aligned} \tau_{xz} = & \int_{c_0}^{c_0+l_b} \left( \frac{ABTx}{\pi} \cdot \exp[A(c-c_0)] \right) \left( \frac{(z-c)^2}{r_1^4} + \frac{(z^2-2cz-c^2)}{r_2^4} + \frac{8cz(z+c)^2}{r_2^6} \right) dc \\ & + \int_{c_0}^{c_0+l_b} \left( \frac{ACTx}{\pi} \cdot \exp[A(c-c_0)] \right) \left( \frac{1}{r_1^2} + \frac{1}{r_2^2} + \frac{4z(z+c)}{r_2^4} \right) dc \\ & + \frac{T}{4\pi a} [\cos 2\theta_2 - \cos 2\theta_1] \end{aligned} \quad (14)$$

where

$$A = \frac{-2\alpha}{d_b}$$

$$B = \frac{1-\nu}{2(1-2\nu)}$$

$$C = \frac{1-3\nu}{4(1-2\nu)}$$

As can be seen, due to the shear stress developed along the anchor bond length, expressions for stress components have integral terms. Integration can be done either analytically, which is a very tedious process, or numerically for a specific problem.

## 5. Illustrative example and verification

### 5.1 Illustrative example

This section investigates in more detail the expressions proposed for analysis of stress by means of an example. This example illustrates the approach proposed for the analysis of rock anchor and provides a sound basis to gain a clear perception of the stress distribution around a tensioned anchor in rock. The formation and extent of compression and tension zones in the rock surrounding the anchor are also discussed in this section.

Due to the complex integral terms in the equations obtained for stress components (Eqs. (12)-(14)), numerical approach has been implemented for evaluating the integrals. The integral terms were approximated to within an error of  $10^{-6}$  using recursive adaptive Lobatto quadrature method (Gander and Gautschi 2000). MATLAB software (Mathworks 2010) was utilized to perform numerical integrations and calculations of stress components.

The tensioned rock anchor problem shown in Fig. 1 was solved using the Eqs. (12-14) obtained in section 4. The various input parameters used in this analysis are given in Table 1. Contour graphs have been used to demonstrate how stresses are distributed around the anchor. Figs. 6 and 7 depict the distribution of vertical stress,  $\sigma_z$ , and horizontal stress,  $\sigma_x$ , around the anchor. In these figures, the horizontal axis is extended along the anchor shaft and the vertical axis corresponds to the rock surface at which the anchor head is installed. In the area of these plots, the positions of bearing plate, unbonded and bond length of the anchor correspond to ( $z = 0, 0 \leq x \leq 0.15$ ), ( $x = 0, 0 < z < 1$ ) and ( $x = 0, 1 \leq z \leq 2$ ), respectively. It should be noted that, due to the geometric symmetry, only half of the anchor problem was studied.

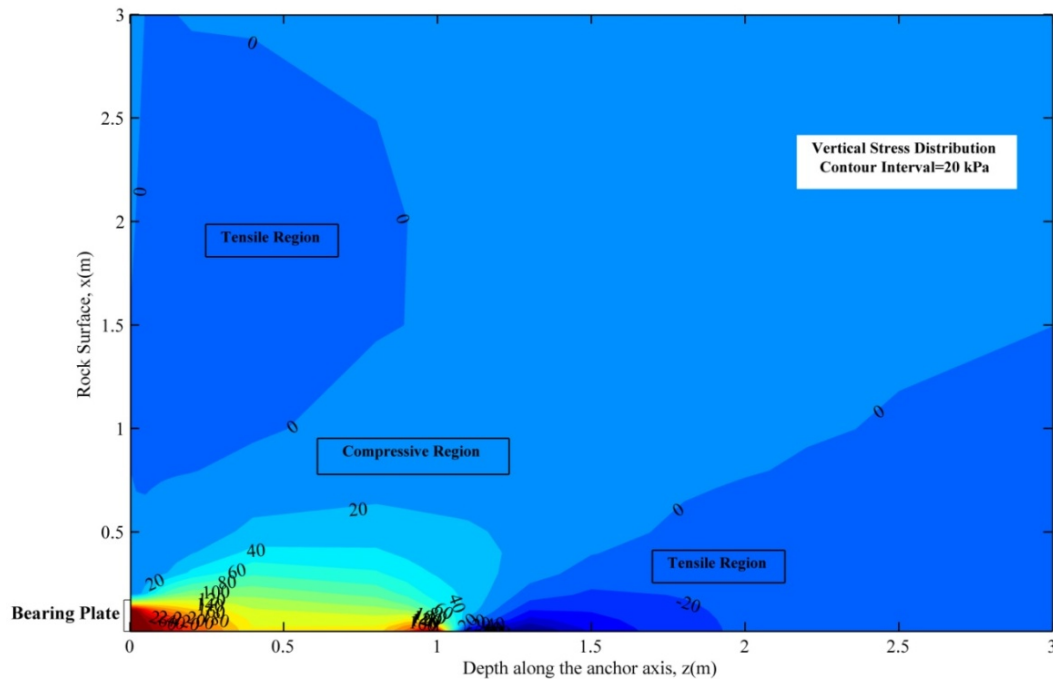
The formation of one compressive and two tensile regions for the vertical stress,  $\sigma_z$ , can be distinguished in Fig. 5. As can be seen, the maximum compressive and tensile values of  $\sigma_z$  are produced beneath the bearing plate and near the proximal end of the bond length, respectively. Fig. 5 shows that the vertical stress is completely compressive in the unbonded region around the anchor axis.

A same region is also observed by Hobst and Zajic (1977) in model tests of a tensioned anchor in sand. This compressive region is of a great importance in providing lateral confinement to the rock and stabilizing the rock near the surface of excavations.

Although  $\sigma_z$  is compressive in the unbonded region, a large tensile stress zone is developed around the anchor bond length especially in the vicinity of the proximal end. Since geo-materials

Table 1 Input parameters used in the example

Bond length, $l_b$	1 m
Unbonded length, $c_0$	1 m
Bearing plate dimension, $2a$	0.3 m
Tension force, $T$	100 kN
Tendon/bar diameter, $d_b$	0.032 m
Grout/drill hole diameter, $d_g$	0.1 m
Young's modulus of rock, $E_r$	30 GPa
Young's modulus of grout, $E_g$	20 GPa
Young's modulus of tendon/bar, $E_b$	200 GPa
Poisson's ratio of rock, $\nu_r$	0.32
Poisson's ratio of grout, $\nu_g$	0.2

Fig. 5 Contours of vertical stress  $\sigma_z$  distribution

generally have low tensile strength, this region with high tensile stress,  $\sigma_z = -110$  kPa, may cause initiation of fractures or even failure of the surrounding rock. That's why; in the design stage, the region surrounding the bond length of a tensioned anchor requires special attention to prevent the failure of rock. In addition to the abovementioned tensile region, another tensile zone away from the anchor axis and near the rock surface (see Fig. 5) is also observed. Due to low values of stress, this tensile region is not considered especially important.

It can be easily deduced from Fig. 6, which depicts the horizontal stress contours, that  $\sigma_x$  distribution is generally similar to that of  $\sigma_z$ . The only exception is that a tensile stress zone with

the maximum value of 17 kPa is formed in the unbonded region far beneath the bearing plate. It is also observed that the compressive stress zone for  $\sigma_x$  is larger in comparison to  $\sigma_z$  and the highest value is also produced under the bearing plate.

Unlike  $\sigma_z$ , the highest value of tensile horizontal stress in the zone near the rock surface outside the bearing plate is considerable and equals to 53 kPa. These tensile stresses in this region which is called the Spalling zone may cause micro-cracking of the surface area. By definition, Spalling stresses are tensile horizontal stresses acting normal to the axis of load and distributed along the loaded rock surface.

Spalling stresses, which are dominated in the Spalling zone, are mainly caused by the condition of compatibility of strains. These stresses are also induced between multiple tensioned anchors along the loaded surface (Windsor 1993). Similar stresses are also observed in the vicinity of the anchorage zone of tensioned concrete members (see for example: Brudent 1990, Sanders and Breen 1997, Zhao *et al.* 2011).

A plot of shear stress distribution,  $\tau_{xz}$ , is shown in Fig. 7. As can be seen, high values of shear stress are produced beneath the edge of bearing plate and in the vicinity of the bond length proximal end. Shear stress concentration under the bearing plate edge can cause punching shear failure of the rock or the reinforcing wall/facing on which the anchor is installed. Note that the concentration of shear stress around the anchor proximal end is mainly due to the shear stresses mobilized at the tendon-grout-rock interfaces (see Fig. 2(b) and Eq. 7). It is worthy of note that shear stress values other than two areas just discussed are small and negligible.

In the following, the effect of relative stiffness between the surrounding rock and the grout,  $r = E_r/E_g$  (stiffness ratio), on the vertical stress is investigated and the results are shown in Fig. 8. In this figure,  $\sigma_z$  variation with depth in the section under the bearing plate ( $x/a = 0.5$ ) is plotted for different values of stiffness ratio,  $r$ , ranging from 0.001 to 5. It is observed that  $\sigma_z$  values

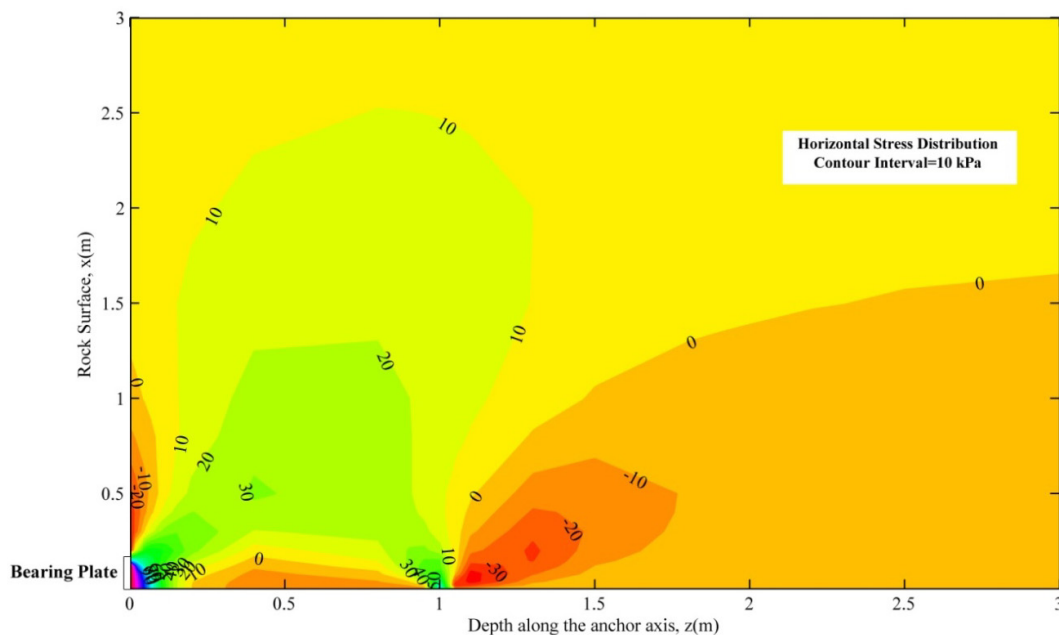


Fig. 6 Contours of horizontal stress  $\sigma_x$  distribution

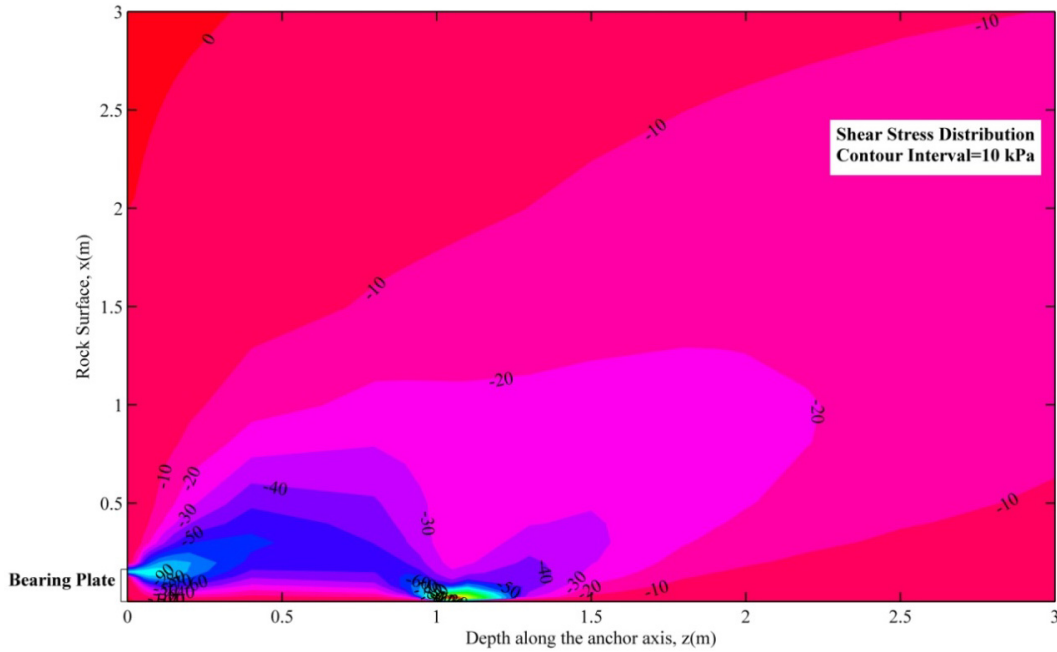


Fig. 7 Contours of shear stress  $\tau_{xz}$  distribution

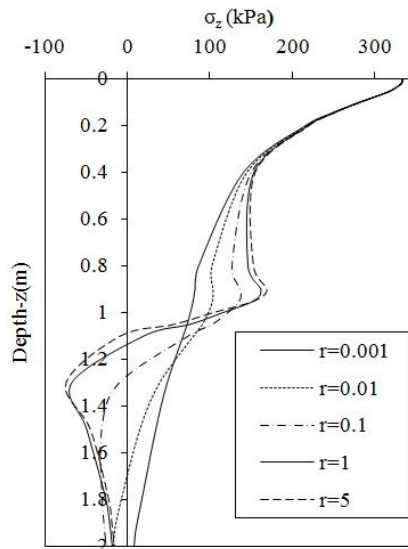


Fig. 8 Variation of  $\sigma_z$  with depth for various relative stiffness between the grout and surrounding rock;  $r = E_r / E_g$

near the bearing plate are similar for various values of  $r$ , but at greater depths, there is a noticeable discrepancy between stress distributions.

What is interesting is that for the smallest value of  $r$  which is valid for soft soils, the vertical stress is completely compressive and no stress concentration is observed with depth. As the

stiffness ratio increases, the curves are separated from each other and large stress concentrations are formed around the proximal end of the anchor bond length.

## 5.2 Verification

In order to verify the results obtained with the outlined analytical approach, the previous example is also solved for with the code FLAC (Itasca Consulting Group, 2005), a 2D Finite Difference Method (FDM) program, with the assumption of plane strain. FLAC uses Cable elements as rockbolt/anchor reinforcements which are capable of modeling the shear resistance between the grout and the cable.

It should be noted that the formulation used in Cable elements does not consider the anchor head (bearing plate) geometry. In order to compare the theoretical results with FDM, it is necessary to consider the anchor head geometry in the FDM code. To simulate the bearing plate in FLAC, the subsequent procedure is followed: In the first step, it is necessary to neutralize the Cable element point load applied to the rock surface. Since the Cable element load is applied to the surface through a node, application of a tensile point load with the same magnitude to this node will counterbalance and neutralize the Cable element load. In the next step, if a distributed pressure corresponding to the stress produced by bearing plate is applied to the rock surface, the bearing plate effect will be correctly modeled with FDM. Moreover, to make a comparison between results obtained from the analytical approach and FDM, the out of plane spacing between rock anchors is taken as unity in FLAC.

Having performed the abovementioned procedure, the stress components are obtained with the FDM. Figs. 9 and 10 show how the stresses obtained with the FDM compare with the analytical approach. It is clearly observed that the analytical results have a very good agreement with FDM. The small discrepancies found near the proximal end can be explained by tensile stress distribution in the tendon embedded in the bond length (Fig. 11). This figure shows that the tensile stress in the tendon near the proximal end in the analytical approach is 20% higher than FDM. This higher tensile stress in the tendon can justify small differences noticed between the stresses obtained by analytical approach and FDM. It should be noted that in the analytical approach the tensile stress

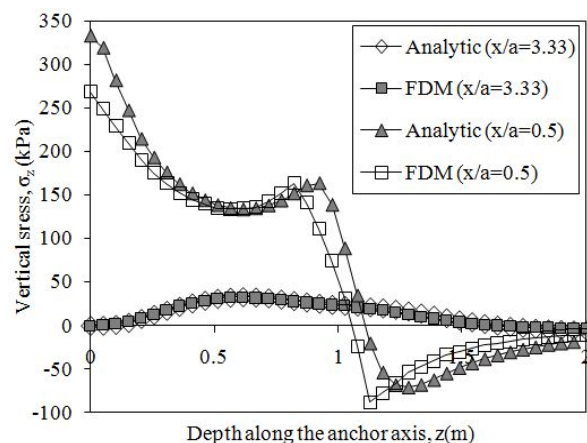


Fig. 9  $\sigma_z$  variation along two vertical sections beneath bearing plate ( $x/a = 0.5$ ) and outside the bearing plate ( $x/a = 3.33$ ). Comparison between FDM and analytical approach

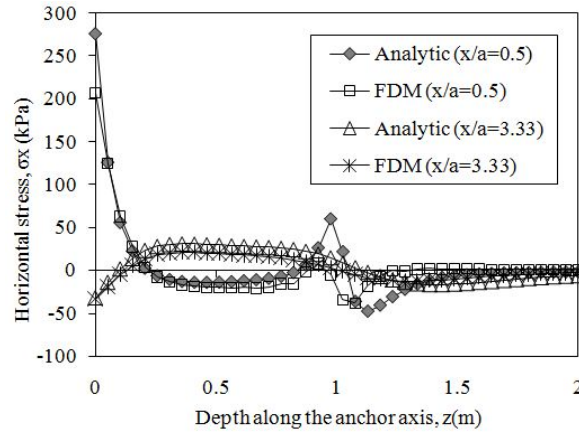


Fig. 10  $\sigma_x$  variation along two vertical sections beneath bearing plate ( $x/a = 0.5$ ) and outside the bearing plate ( $x/a = 3.33$ ). Comparison between FDM and analytical approach

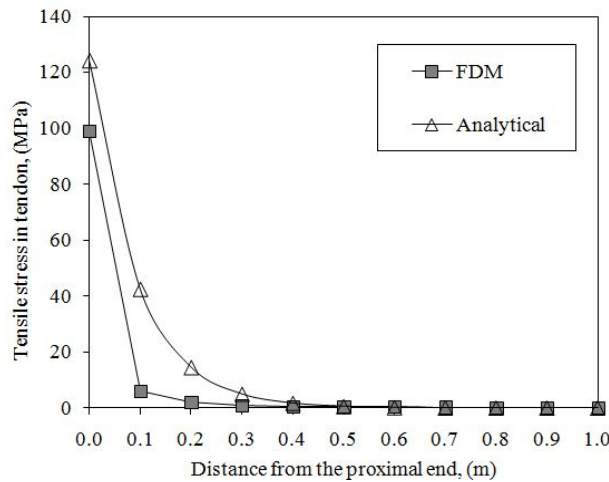


Fig. 11 Tensile axial stress in the tendon embedded in the anchor bond length. Comparison between FDM and analytical approach

in the tendon is obtained from Li and Stillborg (1999) model (Eq. (7)) which has shown good agreement with experiments. Consequently, the results obtained from the analytical approach (white symbols in Fig. 11) are more accurate than those of FDM.

A new theoretical approach for stress analysis around tensioned rock anchors has been developed and presented in this paper. To formulate the problem, a number of assumptions have been made: semi-infinite, isotropic, homogeneous elastic rock; elastic behavior of tendon; plane strain conditions. The problem of stress distribution around a tensioned anchor in rock is solved by decomposing it into two simpler but fundamental problems: A distributed load applied at a finite portion (anchor head area) of the rock surface and a shear stress distribution applied at the interface between the anchor and rock along the grouted bond length. The solution of the first fundamental problem already exists and the solution of the shear stress distributed along the bond length has been found in this paper. The complete solution of the tensioned anchor problem is

obtained according to Superposition principle by addition of the stress components found from the solution of each fundamental problem.

The proposed solution includes details of the anchor head (bearing plate) and grouted bond length. To gain a thorough understanding of the stress distribution around a tensioned anchor in rock, an illustrative example is solved using the proposed formulation and stress contours are drawn for stress components.

Results show that in the unbonded region, the vertical stress is completely compressive and a large tensile zone is formed around the anchor bond length especially in the vicinity of the proximal end. Horizontal stress distribution is found to be generally similar to that of vertical stress but an area of tensile horizontal stress called the Spalling zone is observed outside the face plate near the rock surface. In the case of shear stress, stress concentrations are observed around the bearing plate edge and in the vicinity of the bond length proximal end. Based on the results obtained, large stress concentrations induced around the proximal end of the anchor bond length require special attention in the design stage to prevent initiation and propagation of fractures in rock.

Sensitivity of the vertical stress to the relative stiffness between the grout and surrounding rock was further explored. The results show that for a soft soil/rock the vertical stress is completely compressive and no tensile region is observed around the anchor. As the rock stiffness increases, a tensile region is formed around the anchor bond length and large stress concentrations are observed in the vicinity of the bond length proximal end.

To verify the analytical results, finite difference method (FDM) analysis has been performed and the results are compared with theoretical approach. Very good agreements have been obtained for the analytical results in comparison with FDM. Since a realistic model for distribution of the shear stress along the bond length is assumed in the analytical approach, the accuracy of the proposed solution is higher in comparison to FDM.

The main contributions of this study are consideration of the bearing plate and grouted bond length in derivation of the problem solution. To the knowledge of authors, no studies have been conducted so far that consider bearing plate and bond length in the analysis of stress around tensioned rock anchors. Although the analysis outlined in this paper is novel and has major advantages, the solution has limitations in that it does not consider yielding of the rock and decoupling at the interface between the anchor and the rock. The proposed analytical solution is straightforward and provides accurate values for the stress components. The solution can also be used for preliminary design and calibration of numerical models.

## References

- Akgün, H. and Koçkar, M.K. (2004), "Design of anchorage and assessment of the stability of openings in silty-sandy limestone: A case study in Turkey", *Int. J. Rock Mech. Min. Sci.*, **41**(1), 37-49.
- Bobet, A. (2006), "A simple method for analysis of point anchored rockbolts in circular tunnels in elastic ground", *Rock Mech. Rock. Eng.*, **39**(4), 315-338.
- Bobet, A. and Einstein, H.H. (2011), "Tunnel reinforcement with rockbolts", *Tunn. Undergr. Space Technol.*, **26**(1), 100-123.
- Brown, E.T. (1974), "Fracture of rock under uniform biaxial compression", *Proceedings of the 3rd International Congress on Rock Mechanics*, Denver, CO, USA, September, pp. 111-117.
- Brown, E.T. (Ed.) (1987), *Analytical and Computational Methods in Engineering Rock Mechanics*, Allen & Unwin, London, UK.

- Bruce, D.A. (1992), "Prestressed anchorages for retaining structures applications and construction", ADSC Boston Earth Retention Seminar, Boston, MA, USA.
- Bruce, D.A. (1997), "The stabilization of concrete dams by tensioned rock anchors: the state of American practice", *Proceedings of the International Conference on Ground Anchorages and Anchored Structures*, London, UK, March.
- Brudent, O.L. (1990), "Analysis and design of anchorage zones in post tensioned concrete bridges", Doctor of Philosophy, University of Texas, Austin, TX, USA.
- Culver, R.S. and Jorstad, T. (1967), "Fracturing around a rock bolt anchor", *Proceedings of the 9th US Symposium on Rock Mechanics (USRMS)*, Golden, CO, USA, April.
- Danziger, F.A.B., Danziger, B.R. and Pacheco, M.P. (2006), "The simultaneous use of piles and prestressed anchors in foundation design", *J. Eng. Geol.*, **87**(3-4), 163-177.
- Farmer, I.W. (1975), "Stress distribution along a resin grouted rock anchor", *Int. J. Rock Mech. Min. Sci. Geomech. Abstr.*, **12**(11), 347-351.
- Gander, W. and Gautschi, W. (2000), "Adaptive quadrature – Revisited", *BIT Numer. Math.*, **40**(1), 84-101.
- Gao, F. and Kang, H. (2008), "Effect of pre-tensioned rock bolts on stress redistribution around a roadway-insight from numerical modeling", *J. China Univ. Min. Technol.*, **18**(4), 509-515.
- Hanna, T.H. (1982), *Foundations in Tension-Ground Anchors*, Trans Tech Publications, Clausthal-Zellerfeld, Germany.
- Hobst, L. and Zajic, J. (1977), *Anchoring in Rock*, Elsevier, Amsterdam, Netherlands.
- Hseuh, C.H. (1995), "Modeling of elastic stress transfer in fiber-reinforced composites", *Trends Polym. Sci.*, **10**, 336.
- Itasca Consulting Group, Inc. (2005), *FLAC User's Guide Manual*, (Ver. 5.0), 111 Third Avenue South, Suite 450, Minneapolis, MN 55401, USA.
- Kim, N.K., Park, J.S. and Kim, S.K. (2007), "Numerical simulation of ground anchors", *J. Comput. Geotech.*, **34**(6), 498-507.
- Li, C. and Stillborg, B. (1999), "Analytical models for rock bolts", *Int. J. Rock Mech. Min. Sci. Geomech. Abstr.*, **36**(8), 1013-1029.
- Littlejohn, S. (1993), "Overview of rock anchorages", (Hudson, J.A. Ed.), *Comprehensive Rock engineering, Principles, Practice and Projects*, Pergamon, Volume 4, pp. 413-450.
- Littlejohn, G.S., Norton, P.J. and Turner, M.J. (1977), "A study of rock slope reinforcement at Westfield (Scotland) open pit and the effect of blasting on prestressed anchors", *Proceeding of the Conference on Rock Engineering*, University of Newcastle upon Tyne, UK, April.
- Mathworks, Co. (2010), *Matlab Software*, (Ver. R2010a), Natick, MA, USA.
- McCartney, L.N. (1989), "New theoretical model of stress transfer between fiber and matrix in a uniaxially fiber-reinforced composite", *Proceeding of the Royal Society*, London, UK.
- Mindlin, R.D. (1936), "Force at a point in the interior of a semi-infinite solid", *J. Phys.*, **7**(5), 195-202.
- Muskhelishvili, N.I. (1975), *Some Basic Problem of the mathematical Theory of Elasticity*, (2nd Edition), Noordhoff International Publishing, Netherlands.
- Narin, J.A. and Mendels, D.A. (1996), "On the use of planar shear-lag methods for stress-transfer analysis of multilayered composites", *Mech. Mater.*, **33**(6), 335-362.
- Nitzsche, R.N. and Haas, C.J. (1976), "Installation induced stresses for grouted roof bolts", *Int. J. Rock Mech. Min. Sci. Geomech. Abstr.*, **13**(1), 17-24.
- Papanastassopoulou, F. (1983), "Investigation of effect of rock bolts on stress distribution around underground excavations", *Proceeding of the International Symposium on Rock Bolting*, Abisko, Sweden, August-September.
- Poulos, H.G. and Davis, E.H. (1974), *Elastic Solutions for Soil and Rock Mechanics*, John Wiley and Sons, New York, NY, USA.
- Russell, J.E. (1968), "Stress distribution around rock bolts: Elastic stresses", *Proceedings of the 10th US Symposium on Rock Mechanics (USRMS)*, Austin, TX, USA, May.
- Sabatini, P.J., Pass, D.G. and Bachus, R.C. (1999), "Ground Anchors and Anchored Systems", Office of Bridge Technology Federal Highway Administration (FHWA), Report No. FHWA-IF-99-015.

- Sadd, M.H. (2005), *Elasticity; Theory, Application, and Numerics*, Elsevier Butterworth-Heinemann, Burlington, MA, USA.
- Sagaseta, C., Sanchez, J.M. and Canizal J. (2001), "A general analytical solution for the required anchor force in rock slopes with toppling failure", *Int. J. Rock Mech. Min. Sci.*, **38**(3), 421-435.
- Saliman, R. and Schaefer, R. (1968), "Anchored footings for transmission towers", *ASCE Annual Meeting and National Meeting on Structural Engineering*, Pittsburgh, PA, USA, September-October.
- Sanders, D.H. and Breen, J.E. (1997), "Tensioned anchorage zones with single straight concentric anchorages", *ACI Struct. J.*, **94**(2), 146-158.
- Timoshenko, S.P. and Goodier, J.N. (1970), *Theory of Elasticity*, (3rd Edition), McGraw, New York, NY, USA.
- Tonon, F. and Asadollahi, P. (2008), "Validation of general single rock block stability analysis (BS3D) for wedge failure", *Int. J. Rock Mech. Min. Sci.*, **45**(4), 627-637.
- Wijk, G.A. (1978), "Theoretical remark on the stress field around prestressed rock bolts", *Int. J. Rock Mech. Min. Sci. Geomech. Abstr.*, **15**(6), 289-294.
- Windsor, C.R. (1997), "Rock reinforcement systems", *Int. J. Rock Mech. Min. Sci.*, **34**(6), 919-951.
- Windsor, C.R. and Thompson, A.G. (1993), "Rock reinforcement-technology, testing, design and evaluation", (Hudson, J.A. Ed.), In: *Comprehensive Rock Engineering, Principles, Practice and Projects*, Pergamon, Volume 4, pp. 451-484.
- Wu, Y., Mao, X., Huang, J., Sun, F. and Yao, B. (2010), "Action mechanism of a mechanical end-anchorage bolt", *J. Min. Sci. Technol.*, **20**(4), 625-628.
- Wyllie, D.C. (2005), *Foundations on Rock*, (2nd Edition), Taylor & Francis e-Library.
- Yap, L.P. and Rodger, A.A. (1984), "A study of the behavior of vertical rock anchors using finite element method", *Int. J. Rock Mech. Min. Sci. Geomech. Abstr.*, **21**(2), 47-61.
- Zhao, J.L., Shen, S.H., Wang, L.B. and Chen, J. (2011), "A design approach for the interior anchorage zone of tensioned concrete structures", *KSCE J. Civ. Eng.*, **15**(3), 487-495.

## Appendix A: Derivation of the stresses induced by the anchor bond length

This appendix provides a demonstration of the derivation of the formulations obtained for stresses induced by the shear stresses mobilized along the anchor bond length (See Fig. 2(b)). As stated earlier, the anchor problem can be obtained using two simpler fundamental problems: A uniform distributed load of magnitude  $q$  applied over the surface of the rock under the bearing plate (Fig. 2(a)) and a concentrated force  $P$  applied at a point in the interior of the semi-infinite rock (Fig. 3).

The solutions of the first and the second problems have been presented in Eqs. (1)-(3) and Eqs. (4)-(6), respectively. The latter solution is used to find the stresses induced by the non-uniform distribution of shear stress applied at the interface of the rock-anchor along the bond length.

The shear stress on the interface can be regarded as a concentrated ring load in vertical direction (Fig. 4(a)). The relationship between the force in the tendon inside the bonded zone,  $dF$ , and the shear stress at the interface were obtained as follows (Eq. (11))

$$dF = \frac{2\alpha T}{d_b} \cdot \exp\left(-2\alpha \frac{(c-c_0)}{d_b}\right) dc \quad (\text{A1})$$

The stress components caused by this unit load ring of  $dF$  at an arbitrary point,  $(x,z)$ , in the surrounding rock can be obtained using Eqs. (4)-(6) where  $P$  is replaced by  $dF$  from Eq. (A1). Thus, we have

$$\sigma_x = \frac{-2\alpha T}{\pi d_b} \cdot \exp\left(-2\alpha \frac{(c-c_0)}{d_b}\right) \left[ \frac{1-\nu}{2(1-2\nu)} \left( \frac{(z-c)x^2}{r_1^4} + \frac{(z+c)(x^2+2c^2)-2cx^2}{r_2^4} \right) - \frac{8cz(z+c)x^2}{r_2^6} \right] + \frac{1-3\nu}{4(1-2\nu)} \left( -\frac{(z-c)}{r_1^2} + \frac{z+3c}{r_2^2} - \frac{4zx^2}{r_2^4} \right) dc \quad (\text{A2})$$

$$\sigma_z = \frac{-2\alpha T}{\pi d_b} \cdot \exp\left(-2\alpha \frac{(c-c_0)}{d_b}\right) \left[ \frac{1-\nu}{2(1-2\nu)} \left( \frac{(z-c)^3}{r_1^4} + \frac{(z+c)[(z+c)^2+2cz]}{r_2^4} - \frac{8cz(z+c)x^2}{r_2^6} \right) + \frac{1-3\nu}{4(1-2\nu)} \left( \frac{z-c}{r_1^2} + \frac{3z+c}{r_2^2} - \frac{4zx^2}{r_2^4} \right) \right] \quad (\text{A3})$$

$$\tau_{xz} = \frac{-2\alpha T}{\pi d_b} \cdot \exp\left(-2\alpha \frac{(c-c_0)}{d_b}\right) \left[ \frac{1-\nu}{2(1-2\nu)} \left( \frac{(z-c)^2}{r_1^4} + \frac{(z^2-2cz-c^2)}{r_2^4} + \frac{8cz(z+c)^2}{r_2^6} \right) + \frac{1-3\nu}{4(1-2\nu)} \left( \frac{1}{r_1^2} + \frac{1}{r_2^2} + \frac{4z(z+c)}{r_2^4} \right) \right] \quad (\text{A4})$$

Integration of Eqs. (A.2)-(A.4) with respect to  $dc$  from  $c_0$  to  $c_0 + l_b$  results in the stresses caused by the exponential distribution of shear stress applied along the anchor bond length as follows

$$\sigma_x = \int_{c_0}^{c_0+l_b} \left( \frac{-2\alpha T}{\pi d_b} \cdot \exp\left(-2\alpha \frac{(c-c_0)}{d_b}\right) \right) \left[ \frac{1-\nu}{2(1-2\nu)} \left( \frac{(z-c)x^2}{r_1^4} + \frac{(z+c)(x^2+2cx^2)-2cx^2}{r_2^4} - \frac{8cz(z+c)x^2}{r_2^6} \right) \right] dc - \int_{c_0}^{c_0+l_b} \left( \frac{2\alpha T}{\pi d_b} \cdot \exp\left(-2\alpha \frac{(c-c_0)}{d_b}\right) \right) + \left[ \frac{1-3\nu}{4(1-2\nu)} \left( -\frac{(z-c)}{r_1^2} + \frac{z+3c}{r_2^2} - \frac{4zx^2}{r_2^4} \right) \right] dc \quad (\text{A5})$$

$$\sigma_z = \int_{c_0}^{c_0+l_b} \left( \frac{-2\alpha T}{\pi d_b} \cdot \exp\left(-2\alpha \frac{(c-c_0)}{d_b}\right) \right) \left[ \frac{1-\nu}{2(1-2\nu)} \left( \frac{(z-c)x^2}{r_1^4} + \frac{(z+c)(x^2+2cx^2)-2cx^2}{r_2^4} - \frac{8cz(z+c)x^2}{r_2^6} \right) \right] dc - \int_{c_0}^{c_0+l_b} \left( \frac{2\alpha T}{\pi d_b} \cdot \exp\left(-2\alpha \frac{(c-c_0)}{d_b}\right) \right) + \left[ \frac{1-3\nu}{4(1-2\nu)} \left( \frac{z-c}{r_1^2} + \frac{3z+c}{r_2^2} - \frac{4zx^2}{r_2^4} \right) \right] dc \quad (\text{A6})$$

$$\tau_{xz} = \int_{c_0}^{c_0+l_b} \left( \frac{-2\alpha T}{\pi d_b} \cdot \exp\left(-2\alpha \frac{(c-c_0)}{d_b}\right) \right) \left[ \frac{1-\nu}{2(1-2\nu)} \left( \frac{(z-c)^2}{r_1^4} + \frac{(z^2-2cz-c^2)}{r_2^4} + \frac{8cz(z+c)^2}{r_2^6} \right) \right] dc + \int_{c_0}^{c_0+l_b} \left( \frac{2\alpha T}{\pi d_b} \cdot \exp\left(-2\alpha \frac{(c-c_0)}{d_b}\right) \right) \left[ \frac{1-3\nu}{4(1-2\nu)} \left( \frac{1}{r_1^2} - \frac{1}{r_2^2} + \frac{4z(z+c)}{r_2^4} \right) \right] dc + \frac{T}{4\pi a} [\cos 2\theta_2 - \cos 2\theta_1] \quad (\text{A7})$$